Stability of toroid and rodlike globular structures of a single stiff-chain macromolecule for different bending potentials

Mikhail R. Stukan,[1] Eugeny A. An,[2] Viktor A. Ivanov,[2] and Olga I. Vinogradova[1,3]
[1]*Max Planck Institute for Polymer Research, Ackermannweg 10, 55128 Mainz, Germany*
[2]*Physics Department, Moscow State University, 119992 Moscow, Russia*
[3]*Laboratory of Physical Chemistry of Modified Surfaces, A. N. Frumkin Institute of Physical Chemistry and Electrochemistry, Russian Academy of Sciences, 31 Leninsky Prospect, 119991 Moscow, Russia*
(Received 26 October 2005; published 30 May 2006)

We study the effect of the bending potential on the stability of toroidal and rodlike globules which are typical collapsed conformations of a single stiff-chain macromolecule. We perform numerical calculations in the framework of the bead-stick model of a polymer chain. The intrinsic structure of globules is also analyzed. It was shown that the bending potential affects the packing geometry of bundles in a toroidal globule in the ground state. This potential also influences the bends at the ends of a rodlike globule: both the shape of the loops and the number of bonds in each loop have been investigated numerically as well as by Monte Carlo computer simulations performed for a separate loop. Our main results are (1) the shape of the bending potential could be possibly seen from the geometry of a globule; (2) toroidal globules are always more favorable than the rodlike ones.

DOI: 10.1103/PhysRevE.73.051804 PACS number(s): 82.35.Jk, 82.20.Wt., 82.35.Pq

I. INTRODUCTION

It is well known that many biological macromolecules are globules in their native state, and at the same time many of them, e.g., DNA, can have rather large internal stiffness [1,2]. Controlling DNA condensation is presently of much interest for the development of nonviral approaches to gene therapy [3]. Due to these facts, the ability of a single stiff-chain macromolecule to form different nontrivial globular structures draws a significant attention.

Experimental, theoretical, and computer simulation methods have been widely applied for investigation of stiff-chain polymers. In the experiments several different globular shapes of semiflexible macromolecules have been observed [4–13], including toroidal and rodlike globules. Theoretically, the formation of the so-called small globules by the chains of finite length has been considered more than two decades ago [14]. Different shapes (toroids, cylinders) were predicted depending on the mechanism of flexibility assumed in the model and on the strength of the stiffness potential, as well as monomer-monomer interaction potential [14–25]. The effect of electrostatic interactions (which play an important role in the systems studied experimentally) on the formation of toroidal structures was also calculated [17]. In computer simulation special attention was paid to the conformational behavior of stiff-chain macromolecules [10,26–39]. To sample reasonably large amount of conformations of a single long chain it is necessary to use coarse-grained models, i.e., to consider a chain consisting of monomer units where each unit represents several atoms of a real macromolecule.

In the computer simulation of semiflexible macromolecules a very crucial point is the selection of an appropriate simulation model which includes the choice of bending potential. In this study we use the bead-stick model [40] where the polymer chain is represented as a sequence of beads connected by bonds of fixed length. Most theories use the bending potential proportional to ϑ^2 (ϑ is the angle between two successive bonds along the chain). At the same time, in the computer simulation the typical bending potential is $U_\vartheta \sim 1 - \cos\vartheta$. It is often chosen because of numerical simplicity (it is calculated as the scalar product of bond vectors along the chain) and because it is proportional to ϑ^2 for small angles. However, this $\cos\vartheta$ potential is much "softer" for large angles between successive bonds in comparison to ϑ^2 potential.

In real polymers the bending potential can have a more complicated form, and the problem of a correct definition of a potential is especially significant for biological systems. In fact, there have been some experimental indications in the biological literature that suggest a "high-curvature softening" for DNA [41], and corresponding theoretical models have been also proposed, e.g., kinkable wormlike chain model [42]. Actually, this "softening" can be described by the $\cos\vartheta$ potential considered in the present paper.

It is well known that the phase diagram of model systems depends strongly on the potential used, and, therefore, the understanding of the influence of a particular potential on the appearance of different structures (phases) is important for a comparison with experimental phase diagrams. In this paper we address the issue whether it is possible to use a bending potential of a simple functional form to reproduce wide variety of compact globular structures of stiff-chain polymers observed experimentally. Therefore, here we intentionally consider only bending potential and do not include electrostatic interactions. Another very important question is whether it is possible to extract the form of the bending potential from experimental data, e.g., from observed conformations.

The paper is organized as follows. In Sec. II we describe our model. Section III contains our results for conformational properties of toroidal and rodlike globules for two different bending potentials. Our conclusions are summarized in Sec. IV.

II. MODEL

In our study we use the following model of a polymer chain. A N-mer macromolecule is represented by a sequence of N hard spheres of radius a connected by bond vectors of fixed length $2a$. The angle ϑ between successive bond vectors can take a value between 0 and $2\pi/3$.

To describe stiffness we introduce a bending potential U_ϑ which depends on the angle ϑ. Two different bending potentials have been considered,

$$U_\vartheta^{(1)} = f_1(1-\cos\vartheta) \tag{1}$$

and

$$U_\vartheta^{(2)} = f_2\vartheta^2. \tag{2}$$

The following notation is used below in this paper for the stiffness parameter p:

$$p = \begin{cases} f_1, & U_\vartheta = f_1(1-\cos\vartheta), \\ 2f_2, & U_\vartheta = f_2\vartheta^2. \end{cases} \tag{3}$$

In a coil conformation where all angles are small, for the case $f_1=2f_2$, the behavior of chains with both bending potentials would be almost the same, since their persistence lengths would be equal. But for collapsed globule conformations, where large bending angles exist and an approximation $\cos\vartheta \approx 1-\vartheta^2/2$ cannot be used anymore, a difference in the conformational behavior, based on the type of chosen bending potential, appears. This difference can lead to the fact that for different bending potentials different condensed globular structures are stable. In this paper we focus on an interplay between toroids and rodlike structures as two possible nontrivial globular states of a stiff-chain macromolecule.

The volume interaction between monomer units of the chain is taken into account by means of estimation of a surface energy of the globule E_{surf}. For this purpose we introduce a surface tension parameter γ, which characterizes a penalty per one exposed contact which have monomers at the surface of the globule. Then the surface energy could be calculated as the number of exposed contacts, n_{exp}, multiplied by γ,

$$E_{\text{surf}} = \gamma n_{\text{exp}}.$$

To confirm our numerical calculations of the shape of loops in a rodlike globule we perform Monte Carlo simulations, however, only for a part of the chain, namely, for one separated loop. In our computer simulations we use the off-lattice bead-stick model which is very similar to the model used in numerical studies. In order to describe the interaction of nonbonded monomer units separated by the distance r we have chosen the following potential:

$$U_{\text{NB}} = \begin{cases} \infty, & r < 2a, \\ -2\gamma, & 2a \le r \le 2a+\delta r, \\ 0, & r > 2a+\delta r, \end{cases} \tag{4}$$

where a is the radius of one monomer unit ($2a$ is equal to one unit length) and the parameter δr was chosen to be equal to $\delta r=0.01$. We have also performed simulations at the values $\delta r=0.02$ and 0.005, and we have found that the choice of this parameter does not influence the equilibrium shape of the loop. The bending potential between two successive bond vectors along the chain is given by Eq. (1) or by Eq. (2). We have performed simulation at the following values of parameters: stiffness parameter $p=250$, parameter γ was varied from 5 up to 50, so the ratio γ/p was varied from 0.02 to 0.2.

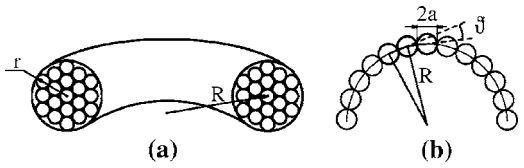

FIG. 1. A toroidal globule with the hexagonal packing of circuits (a). Bending angles inside a circuit (b).

In our simulation the temperature was equal to $k_BT=0.3$ because we were interested in finding the ground state, and therefore wanted to diminish the effects of entropy in the simulation. With our parameters, the contribution of thermal fluctuations is negligibly small.

In each Monte Carlo step, two monomer units are chosen at random and the whole part of the chain between them is rotated arbitrarily around the connecting axis. For this trial conformation it is checked whether the excluded volume condition is fulfilled, and afterwards this trial step is accepted with the usual Metropolis rate. This kind of Monte Carlo steps ensures that the length of each bond along the chain remains constant during the simulation and thus the requirement of the bead-stick model is fulfilled.

III. RESULTS AND DISCUSSION

A. Toroidal globule

The first nontrivial globular structure which we consider is a toroidal globule. It is characterized by its radius R and radius of its cross section r [see Fig. 1(a)]. In our calculations we suppose $R \gg r$ (the case of an ideal toroid, later we will check the validity of such an approximation). It means that we consider the bending angle between adjacent bonds to be constant along the chain $\vartheta \approx \frac{2a}{R}$ [see Fig. 1(b)] (more precisely, angle values are distributed in the interval $\frac{2a}{(R-r)} < \vartheta < \frac{2a}{(R+r)}$ and depend on the location of the particular filament in the bundle).

Toroids or other collapsed structures of stiff-chain macromolecules are formed due to the interplay between the bending energy E_ϑ and the surface energy E_{surf}, and correspond to the minimum of the total energy $E_{\text{total}}=E_\vartheta+E_{\text{surf}}$.

In the limit $R \gg r$ the bending energy of a toroidal globule E_ϑ^{tor} is

$$E_\vartheta^{\text{tor}} = (N-1)U_\vartheta\left(\frac{2a}{R}\right). \tag{5}$$

Here $U_\vartheta\left(\frac{2a}{R}\right)$ is a value of a bending potential which corresponds to the angle $\frac{2a}{R}$.

To estimate the surface energy E_{surf} we must calculate the number of exposed contacts for a particular globular confor-

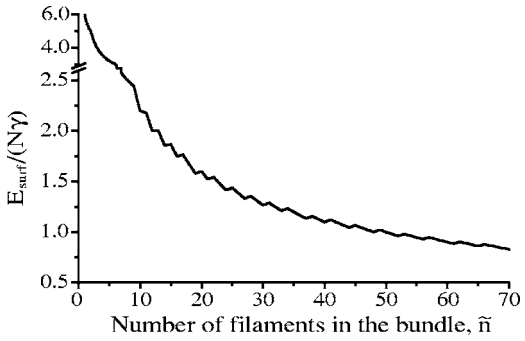

FIG. 2. Surface energy per monomer unit as a function of number of filaments in a bundle with hexagonal packing.

mation, n_{exp}. This number of course depends on the packing of monomers in the globule. As it was pointed out by Ubbink and Odijk [17], the packing of filaments in the toroidal bundle can be considered to be a hexagonal, which is the limit of a toroidal crystal and is observed for condensed structures [43]. Let us introduce now the parameter $A^{(n)}$—the number of exposed contacts per one slice of toroid's cross section of the width equal to the size of one monomer unit (length is measured in monomer diameters $2a$) for a bundle of n filaments with hexagonal packing [24]:

$$A^{(n)} = 12\mathcal{W}_{(n)} - 6 + 2(1 - \delta_{\mathcal{C}_{(n)},0}) + 2\mathcal{J}\left(\frac{\mathcal{C}_{(n)}}{\mathcal{W}_{(n)}}\right),$$

where $\mathcal{W}_{(n)} = \mathcal{J}\left[\frac{3+\sqrt{12n-3}}{6}\right]$, $\mathcal{C}_{(n)} = n - 3\mathcal{W}_{(n)}^2 + 3\mathcal{W}_{(n)} - 1$, $\mathcal{J}[x]$ is the largest integer not greater than x and δ_{ij}—Kroneker delta.

In the general case the number of circuits in a toroid can be characterized by a noninteger number $\tilde{n}$ in the following way: $\tilde{n} - n$ part of a toroid consists of $n+1$ circuits while the rest part consists of n circuits ($0 \le \tilde{n} - n < 1$). Consequently, the surface energy of the toroidal globule E_{surf}^{tor} can be written as

$$E_{surf}^{tor} = \frac{\gamma}{2a}\{2\pi R(\tilde{n} - n)A^{(n+1)} + 2\pi R[1 - (\tilde{n} - n)]A^{(n)}\}. \quad (6)$$

Since $2\pi R\tilde{n} = 2Na$, Eq. (6) can be rewritten as

$$E_{surf}^{tor} = N\gamma\left(\frac{(\tilde{n} - n)}{\tilde{n}}A^{(n+1)} + \frac{[1 - (\tilde{n} - n)]}{\tilde{n}}A^{(n)}\right). \quad (7)$$

And the total energy of the toroidal globule is

$$E_{total}^{tor} = E_{\vartheta}^{tor} + E_{surf}^{tor} = (N-1)U_{\vartheta}\left(\frac{2\pi\tilde{n}}{N}\right) + N\gamma\left(\frac{(\tilde{n} - n)}{\tilde{n}}A^{(n+1)} + \frac{[1 - (\tilde{n} - n)]}{\tilde{n}}A^{(n)}\right). \quad (8)$$

As it was shown in Ref. [24] only toroidal globules comprised of particular number of circuits are stable. This effect comes from the fact that the surface energy of the toroidal globule [see Eq. (7)] considered as a function of $\tilde{n}$ has local minima, which, for $n > 5$, correspond to toroidal globules with integer number of circuits ($\tilde{n} = n$) (see Fig. 2). The surface energy function has singular points in these minima. Since the bending energy is a monotonic function of $\tilde{n}$, the total energy of a toroidal globule E_{total}^{tor} has singular points exactly at the same values of $\tilde{n}$ as the surface energy E_{surf}^{tor}. One of these singular points becomes a global minimum for the total energy (because the main term in the surface energy is $\tilde{n}^{-1}$ while the bending energy increases proportionally to $\tilde{n}^2$).

These "magic" numbers of filaments, which correspond to the local minima of the surface energy, and corresponding $A^{(n)}$ for the number of filaments up to the first five complete hexagonal shells are presented in Table I. (Complete shells contain 7, 19, 37, 61, 91 circuits, respectively, and are marked in boldface type in Table I).

Figure 3 shows maps in chain length—stiffness coordinates for different values of parameter γ. The chain length is measured in number of monomers in the chain N, and the stiffness is determined by the parameter p [Eq. (3)]. Different colors show how many circuits have the toroidal conformation with the lowest energy. This number of circuits corresponds to the minimum of the total energy [Eq. (8)] for a chain with particular N and p at a given value of γ. These maps were built for chains with both bending potentials: $U_{\vartheta} \sim (1 - \cos\vartheta)$ and $U_{\vartheta} \sim \vartheta^2$, but in Fig. 3 we present only the pictures for $U_{\vartheta} \sim (1 - \cos\vartheta)$. The reason is that the maps for both bending potentials are almost undistinguishable.

White color in Fig. 3 marks the area where toroidal structure cannot exist. What does it mean? It is evident that we cannot talk about any "toroidality" for a structure with $r > R$ (see Fig. 1). This criterion can be written as

$$N > \pi\tilde{n}\sqrt{\tilde{n}}.$$

Here we take into account that for an ideal toroid $R = \frac{Na}{\pi\tilde{n}}$ and the radii of its cross section can be estimated as $r \approx a\sqrt{\tilde{n}}$.

TABLE I. "Magic" numbers of filaments which correspond to the local minima of toroidal globule's total energy [see Eq. (8)]. Numbers printed in boldface type correspond to complete shells.

n	**7**	10	12	14	16	**19**	21	24	27	30	33	**37**
$A^{(n)}$	**18**	22	24	26	28	**30**	32	34	36	38	40	**42**
n	40	44	48	52	56	**61**	65	70	75	80	85	**91**
$A^{(n)}$	44	46	48	50	52	**54**	56	58	60	62	64	**66**

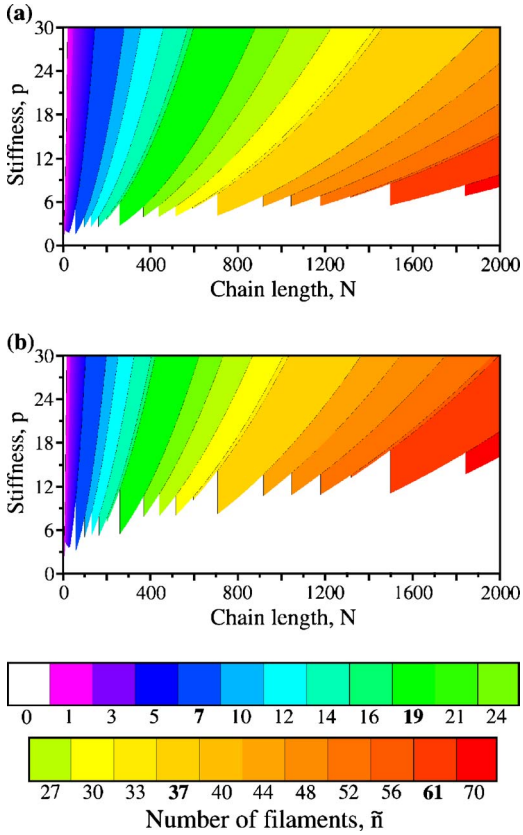

FIG. 3. (Color online) The maps of stability of toroidal structures in coordinates of the chain length—stiffness for the stiffness potential $U_\vartheta \sim (1-\cos\vartheta)$, $\gamma=1.0$ (a) and 2.0 (b). Colors indicate the number of filaments in the toroid which is stable at given values of parameters.

As it can be seen from Fig. 3, the parameter γ influences the map significantly. Nevertheless, as it was shown by Pereira and Williams [24], if the number of filaments in the equilibrated toroidal structure is considered as a function of a renormalized chain length $\mathcal{N} \equiv N\sqrt{\frac{\gamma}{p}}$, the corresponding dependence $\tilde{n}(\mathcal{N})$ is uniform for all γ.

A comparison of these dependencies for toroids with bending potentials $U_\vartheta \sim (1-\cos\vartheta)$ and $U_\vartheta \sim \vartheta^2$ confirms that, in the approximation of an ideal toroid, the influence of the type of the bending potential is negligible and can be seen only for large $\mathcal{N}$ (Fig. 4).

B. Nonideal toroids

In the preceding section we have analyzed the stability of toroidal structures in the approximation of an ideal toroid. In the current section we explore how correct this approximation is and how significant would be the changes if we take into account some nonideal effects in bending energy since in a real toroidal globule different filaments have different curvature radii. For simplicity we consider toroids with the number of circuits equal to 7, 19, 37, and 61. These numbers of filaments correspond to the cases of filled first, second, third, and fourth hexagonal shell, respectively (see Fig. 5).

Since now we do not consider all the circuits to be of similar radius R, the bending energy of the globule can no longer be expressed by Eq. (5).

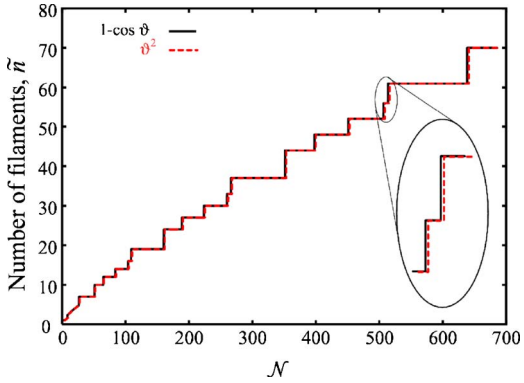

FIG. 4. (Color online) Number of circuits in a toroid $\tilde{n}$ vs renormalized chain length $\mathcal{N}$ for bending potentials: $U_\vartheta \sim (1-\cos\vartheta)$ and $U_\vartheta \sim \vartheta^2$.

Let us estimate the bending energy for a nonideal toroidal structure. The bundle with hexagonal order of filaments can orient in respect to axis of toroid in many different ways, but there are two limiting cases [see Figs. 5(a) and 5(b)], which we have analyzed (all other orientations are intermediate between these two).

Let us introduce the following notation: n_k—the number of filaments in a toroid composed of k filled hexagonal shells ($k=1 \leftrightarrow n_k=7$; $k=2 \leftrightarrow n_k=19$; $k=3 \leftrightarrow n_k=37$; $k=4 \leftrightarrow n_k=61$). Then for the case (a) (see Fig. 5) the bending energy of a nonideal toroidal globule of n_k filaments can be written as

$$E_\vartheta^{(n_k)} = \left(\frac{(2k+1)N}{n_k} - 1\right) U_\vartheta\left(\frac{2\pi n_k}{N}\right) + \sum_{j=1}^{k} (2k+1-j)\left(\frac{N}{n_k} \pm j\pi\sqrt{3}\right) U_\vartheta\left(\frac{2\pi n_k}{N \pm j\pi n_k\sqrt{3}}\right). \tag{9}$$

And for the case (b) (see Fig. 5),

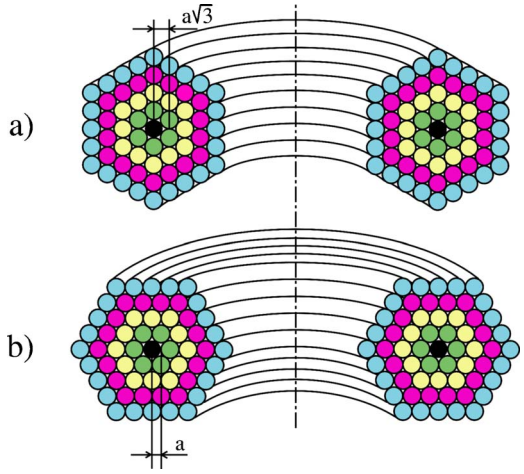

FIG. 5. (Color online) Two different orientations of the hexagonal bundle in the toroidal globule. (Orientation of hexagonal bundle differs for 30°. Different colors correspond to different hexagonal shells.)

$$E_{\vartheta}^{(n_k)} = \left(\frac{\left[2\mathcal{J}\left(\frac{k}{2}\right) + 1 \right] N}{n_k} - 1 \right) U_{\vartheta}\left(\frac{2\pi n_k}{N}\right) + \sum_{j=1}^{k} j \left(\frac{N}{n_k} \pm (2k+1-j)\pi \right) U_{\vartheta}\left(\frac{2\pi n_k}{N \pm (2k+1-j)\pi n_k} \right) + \sum_{j=1}^{k} \left[2k - 2\mathcal{J}\left(\frac{k}{2}\right) + (-\delta_{j,2\mathcal{J}(j/2)})^{1+\delta_{k,2\mathcal{J}(k/2)}} \right] \times \left(\frac{N}{n_k} \pm j\pi \right) U_{\vartheta}\left(\frac{2\pi n_k}{N \pm j\pi n_k} \right), \quad (10)$$

where $\mathcal{J}[x]$, as before, is the largest integer not greater than x.

It can be easily seen that the bending energy is different for these two conformations. Moreover the case (a) is much more favorable for a chain with the bending potential $U_{\vartheta} \sim \vartheta^2$ while the case (b) corresponds to the minimum of the bending energy for a chain with $U_{\vartheta} \sim (1-\cos\vartheta)$. For both potentials the difference in energy between toroidal structures with different packing of bundles becomes more pronounced for thicker toroids. This observation is very important. It indicates that the bending potential influences the spatial arranging of filaments inside a globule.

We have analyzed the ratio $E_{\vartheta}(\text{nonid})/E_{\vartheta}(\text{id})$ for 7-, 19-, 37-, and 61-circuit toroids, where $E_{\vartheta}(\text{id})$ is the bending energy of an ideal toroid [calculated according to Eq. (5)], and $E_{\vartheta}(\text{nonid})$ is the bending energy of nonideal ones [Eqs. (9) for $U_{\vartheta} \sim \vartheta^2$ and (10) for $U_{\vartheta} \sim (1-\cos\vartheta)$, respectively]. It was found that the total energy calculated for a nonideal toroid is always larger than that for an ideal toroidal structure. The ratio $E_{\vartheta}(\text{nonid})/E_{\vartheta}(\text{id})$ becomes larger with the increase in the number of filaments in the toroidal globule, and for relatively "thick" toroids it exceeds 1.1. The type of bending potential plays very important role as well. In Fig. 6 we present the ratio $E_{\vartheta}(\text{nonid})/E_{\vartheta}(\text{id})$ for $\gamma=1.0$, which illustrates very well that nonideal effects are much more pronounced for the case of bending potential $U_{\vartheta} \sim \vartheta^2$ than for $U_{\vartheta} \sim (1-\cos\vartheta)$.

We remark that although it is known that for some values of surface tension and stiffness the most favorable is a state of "twisted" toroid, where individual filaments lower their bending energy by additionally orbiting around the mean path along which they wind [44], these structures cannot be observed in most real experiments because of the kinetic reasons. There are also experimental evidences and theoretical models for other types of filament packing in toroids, e.g., circumferential wrapping [45,46]. In our study we do not take into account the above-mentioned effects as well as any other possible defects, e.g., quenched or inevitable structural defects caused by chain connectivity [47], and consider only nontwisted toroidal structures with coplanar concentric loops.

C. Rodlike globule

The second type of a condensed structure which can be formed by a stiff-chain macromolecule is a rodlike globule.

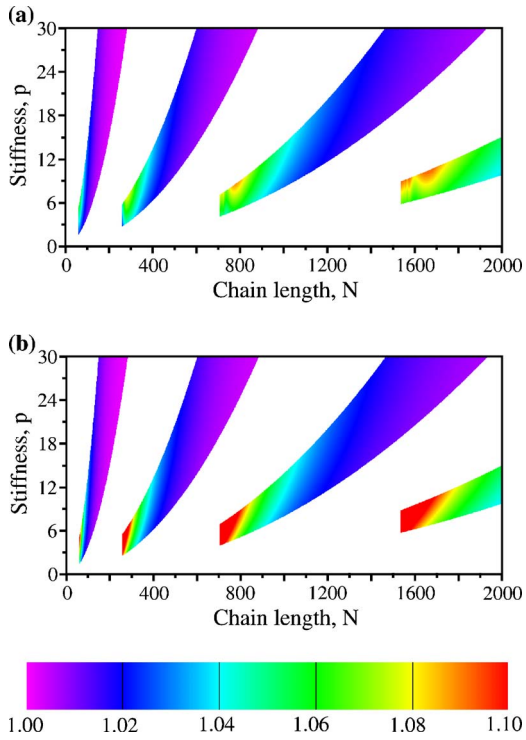

FIG. 6. (Color online) The maps of ratio $E_{\vartheta}(\text{nonid})/E_{\vartheta}(\text{id})$ for toroids of 7, 19, 37, 61 filaments in variables of the chain length—stiffness for bending potentials $U_{\vartheta} \sim (1-\cos\vartheta)$ (a) and $U_{\vartheta} \sim \vartheta^2$ (b), in both cases $\gamma=1.0$.

An example of a perfectly ordered rodlike structure is shown in Fig. 7. Here we still assume that in a 3D space the hexagonal packing is the most favorable one. In our study we consider rodlike globules consisting of several filaments of the same length, H, and one filament of a length equal to or less than H. (We simplify the picture. In principle, the globule can have two filaments with the length less than H, but, as can be easily seen, the surface energy of such a structure is higher while the bending energy is the same as in the case of one shortened filament. This means that such a conformation should be unfavorable.)

In the standard bead-stick chain model, rodlike structures can be formed with loops at the ends (such structures were called "racquets" in Ref. [39]) or without them. We first analyze the formation of the bends. It is obvious that the bending on 180 degrees can be performed by different ways and a different number of monomers can be involved in this process. Let us consider some of these bends to find which of them correspond to the equilibrium states for both bending potentials [$U_{\vartheta} \sim (1-\cos\vartheta)$ and $U_{\vartheta} \sim \vartheta^2$]. For this purpose we considered a single filament and study the shape of the loop between points A and B which separate the bend from

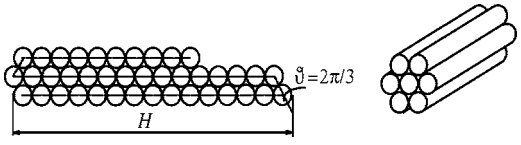

FIG. 7. "Perfect" rodlike globule.

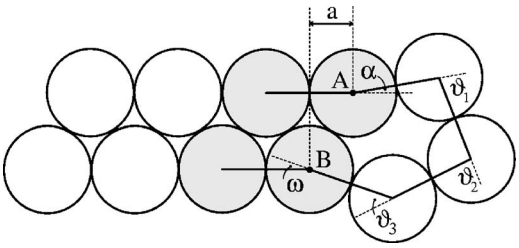

FIG. 8. A bend of a chain in a rodlike globular state.

the perfectly ordered part of the rod (see Fig. 8). We varied the number of bonds between points A and B from 3 to 12 (which means that the considered bends are formed by m monomers, $4 \le m \le 13$). Corresponding bending energies and the equilibrium shapes of the bends are shown in Table II.

The values and shapes in Table II were obtained by numerical minimization of the bending energy E_ϑ:

$$E_\vartheta = U_\vartheta(\alpha) + \sum_{i=1}^{m-2} U_\vartheta(\vartheta_i) + U_\vartheta(\omega), \tag{11}$$

taking into account the following constraints:

$$\alpha - \sum_{i=1}^{m-2} \vartheta_i + \omega = -180^\circ,$$

$$AB = 2a, \quad A_x - B_x = a,$$

where m is the number of monomers which form the bend (between points A and B).

TABLE II. Equilibrium shapes (for definition of angles $\alpha, \vartheta_1, \ldots, \vartheta_{10}, \omega$ see Fig. 8) and corresponding bending energies, E_ϑ, of the bends consisted of m monomers. Data for $U \sim (1-\cos\vartheta)$ potential are shown in normal style while those for $U \sim \vartheta^2$ potential are shown in italic. Two methods have been used—numerical minimization (NM) and Monte Carlo simulations (MC). For a definition of $(\gamma/p)^*$ see the text. Values for E_ϑ are given in energetic units, the values for angles are given in degrees (not in radians).

m	4	5	6	7	8	9	10	11	12
method	NM/MC	NM/MC	NM/MC	NM/MC	NM/MC	NM/MC	NM/MC	NM/MC	NM/MC
E_ϑ	2.000/2.001	1.893/1.895	1.840/1.844	1.729/1.735	1.623/1.631	1.515/1.525	1.415/1.427	1.325/1.334	1.243/1.256
	5.209/5.213	*4.720/4.726*	*4.276/4.286*	*3.877/3.889*	*3.536/3.553*	*3.243/3.262*	*2.991/3.014*	*2.774/2.800*	*2.584/2.611*
α	0.0/1.3	−11.8/−12.0	6.5/6.6	6.5/6.5	10.9/12.0	12.2/12.1	13.1/13.0	13.5/12.4	13.7/13.3
	−15.0/−14.9	−2.3/−2.3	*6.5/6.6*	*10.5/10.5*	*12.8/13.4*	*13.9/13.8*	*14.4/14.4*	*14.6/14.6*	*14.5/14.7*
ϑ_1	120.0/119.4	48.9/48.7	24.5/24.9	20.4/20.6	11.7/13.7	7.0/7.0	3.2/3.6	0.5/2.3	−1.5/−1.3
	105.0/105.1	*65.0/65.1*	*39.4/39.4*	*24.2/23.9*	*14.4/14.4*	*8.1/8.2*	*3.7/3.9*	*0.7/2.6*	*−1.5/−2.7*
ϑ_2	60.0/60.6	117.1/117.2	100.8/100.4	53.8/53.4	37.8/36.4	27.7/27.7	20.1/20.6	14.6/13.7	10.5/8.6
	75.0/74.9	*96.3/96.3*	*82.2/82.2*	*60.3/60.6*	*43.2/43.9*	*30.9/30.8*	*22.2/22.5*	*16.0/16.4*	*11.4/11.2*
ϑ_3		16.6/16.7	58.2/58.5	90.4/90.9	74.4/75.3	53.0/53.2	39.8/39.3	30.5/28.7	23.6/24.1
		38.6/38.6	*68.2/68.3*	*74.6/74.7*	*65.8/65.5*	*53.0/53.0*	*41.5/41.6*	*32.2/32.3*	*25.0/25.4*
ϑ_4			18.1/18.0	34.9/34.7	58.1/56.4	66.6/66.4	58.6/58.8	47.4/47.5	38.0/39.2
			21.0/20.9	*46.1/46.0*	*58.9/58.4*	*60.3/60.4*	*54.6/54.7*	*46.4/46.2*	*38.3/38.0*
ϑ_5				6.5/6.3	26.9/28.1	41.6/41.7	51.9/51.6	53.7/56.7	48.8/48.7
				10.0/9.9	*31.3/31.9*	*44.6/44.8*	*50.7/49.9*	*50.5/50.3*	*46.5/47.0*
ϑ_6					2.8/3.8	18.4/18.4	31.1/31.1	40.4/41.2	45.3/43.8
					3.3/3.0	*21.3/21.2*	*33.5/33.7*	*41.1/41.4*	*44.1/44.1*
ϑ_7						−1.1/−2.4	12.7/13.2	23.4/20.5	31.8/33.6
						−1.0/−2.6	*14.3/15.1*	*25.3/25.5*	*32.9/32.7*
ϑ_8							−3.6/−3.9	8.4/8.1	17.8/17.3
							−3.8/−4.2	*9.4/9.3*	*19.1/19.5*
ϑ_9								−5.4/−5.8	5.3/4.8
								−5.7/−5.8	*5.9/5.7*
ϑ_{10}									−6.6/−5.9
									−7.0/−7.1
ω	0.0/1.3	14.4/14.5	15.0/15.1	19.5/19.3	20.6/21.3	20.9/21.0	20.5/21.0	20.0/18.8	19.3/19.8
	15.0/14.9	*22.2/22.2*	*24.3/24.2*	*24.7/24.4*	*24.2/23.6*	*23.3/23.0*	*22.3/22.6*	*21.3/21.4*	*20.3/19.9*
$(\frac{\gamma}{p})^*$	0	0.0269	0.0267	0.0338	0.0377	0.0404	0.0418	0.0422	0.0421
	0.0685	*0.0954*	*0.1006*	*0.1004*	*0.0974*	*0.0934*	*0.0890*	*0.0847*	*0.0805*
$1-\cos\vartheta$	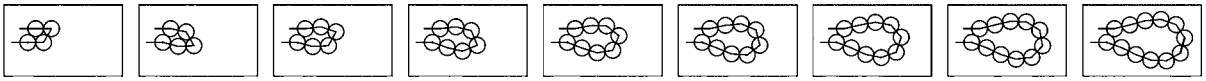								
ϑ^2	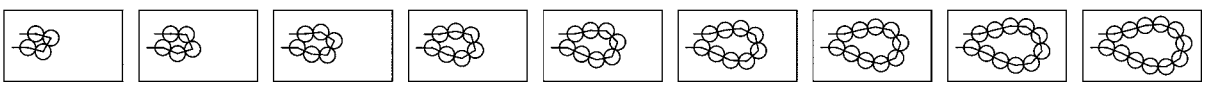								

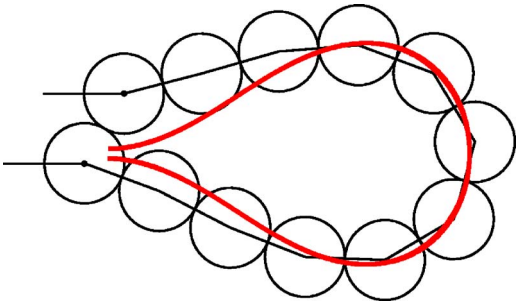

FIG. 9. (Color online) Comparison of numerical solution with *elastica*.

Each trivial bend (see Fig. 7) contributes the value $2.000f_1$ or $5.483f_2$ to the total energy for $U_\vartheta = f_1(1-\cos\vartheta)$ and $U_\vartheta = f_2\vartheta^2$, respectively. If the chain forms a bend of a "nontrivial" form (as can be seen in Table II) it can decrease its bending energy (note that for calculation of the energy in Table II we used $f_1 = f_2 = 1$), but at the same time the number of empty places for contacts becomes larger and the surface energy increases. Until the loss in surface energy is larger than the gain in bending energy the chain will form trivial bends (as it is shown in Fig. 7). The values of ratio $(\gamma/p)^*$, below which the corresponding type of the bend is more favorable than the trivial one, are shown in Table II.

We have compared our numerical results to the very similar analysis of so-called "racquets" made in Ref. [39] where an analytical result for the harmonic potential was provided and the *elastica* shape has been obtained (for the case of infinitely thin chain). As can be seen from Fig. 9 the shape of the loop in our numerical calculations coincides rather well with *elastica*.

To confirm the results of the numerical minimization we have also performed Monte Carlo simulations. We have considered a simple rod with one bend (see Fig. 8). To simulate the existence of a perfectly ordered part of the rod near the bend we fixed four monomer units (two at each end of the chain, the fixed monomer units are filled with gray in Fig. 8) and we did not consider the rest of the monomer units in the straight part of the globule (where filaments are perfectly ordered). Though such a constraint looks a little artificial it is suitable for the studied problem (determination of the shape of the loop). The number of bonds between points A and B in the loop was varied from 3 to 12 and we have analyzed the shape of the corresponding bend. The interaction potential between nonbonded monomer units is given by Eq. (4).

Starting from a random conformation (with four fixed beads at the ends) we have performed in each simulation a series of Monte Carlo steps, accepted or rejected according to the Metropolis algorithm. As it was mentioned above in each Monte Carlo update, two monomer units are chosen at random (except the first and the last monomers at the ends) and the part of the chain between them is rotated randomly around the axis connecting them.

As can be seen from Table II results of the simulations agree well with the numerical estimates. But not all the structures shown in Table II can be observed because some of them do not correspond to the minimum of total energy at any (γ/p). Which type of the bend is the most favorable one

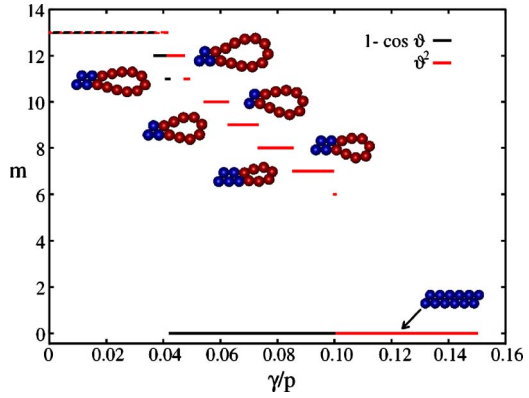

FIG. 10. (Color online) Structure of bends in a rodlike globule for two bending potentials $[U_\vartheta \sim (1-\cos\vartheta)$ and $U_\vartheta \sim \vartheta^2]$. The dashed line at $m=13$ means that we did not consider bends with $m>13$ and cannot say where this bend $(m=13)$ becomes unstable.

at particular value of (γ/p) is shown in Fig. 10. As can be seen there is a significant difference between the chains with bending potential $U_\vartheta \sim (1-\cos\vartheta)$ and $U_\vartheta \sim \vartheta^2$. For the case of $U_\vartheta \sim \vartheta^2$ the variety of possible bends which can be stable is bigger, though for this case a trivial bend $(m=0)$ becomes unstable at higher values of γ/p.

Here we consider perfect rods only, i.e., we consider our chains in the area where $\gamma/p > (\gamma/p)^{\text{trivial}}$, here $(\gamma/p)^{\text{trivial}}$ is the largest value of $(\gamma/p)^*$ (see Table II), $(\gamma/p)^{\text{trivial}} = 0.0422$ for $U_\vartheta \sim (1-\cos\vartheta)$ and $(\gamma/p)^{\text{trivial}} = 0.1006$ for $U_\vartheta \sim \vartheta^2$.

Since the number of filaments in the bundle, $\tilde{n}$, gives the major influence on the surface energy, the "favorable" numbers of filaments for rod and toroid are the same (see Table I) and depend on the packing structure only, which, as previously, is supposed to be hexagonal. As for toroidal globule the total energy of rodlike globule $E_{\text{total}}^{\text{rod}}$ consists of two parts: surface energy $E_{\text{surf}}^{\text{rod}}$ and bending energy E_ϑ^{rod}. Since we consider here only perfectly ordered rodlike globules (example of such a structure can be seen in Fig. 7) then

$$E_{\text{surf}}^{\text{rod}} = N\gamma\left(\frac{(\tilde{n}-n)}{\tilde{n}}A^{(n+1)} + \frac{[1-(\tilde{n}-n)]}{\tilde{n}}A^{(n)}\right) + 2n\gamma \tag{12}$$

and

$$E_\vartheta^{\text{rod}} = n'\left[U_\vartheta\left(\frac{2\pi}{3}\right) + U_\vartheta\left(\frac{\pi}{3}\right)\right], \tag{13}$$

where

$$n' = \begin{cases} n-1, & \tilde{n} = n, \\ n, & \text{otherwise}. \end{cases}$$

(Definition of $\tilde{n}$ is the same as for the toroidal globule above.)

The total energy for a rodlike structure is

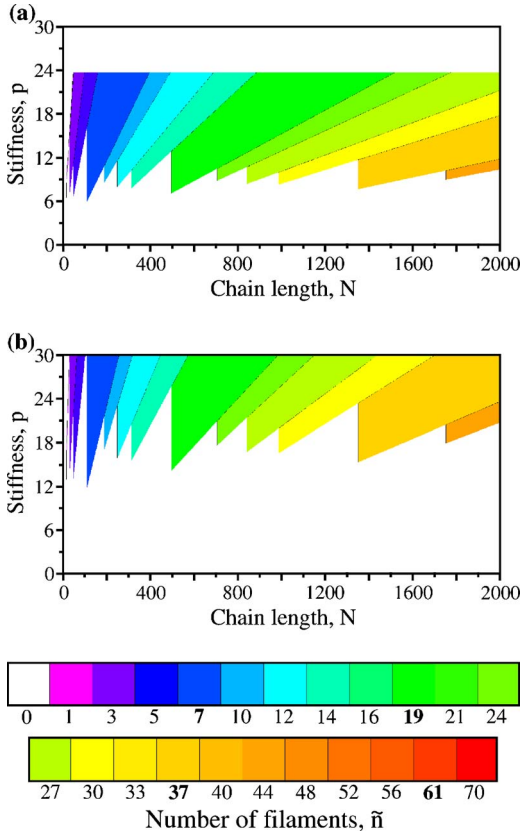

FIG. 11. (Color online) The maps of stability of perfect rodlike structures (with trivial bends) in variables of the chain length—stiffness for stiffness potential $U_\vartheta \sim (1-\cos\vartheta)$, $\gamma=1.0$ (a), $\gamma=2.0$ (b). The color indicates the number of filaments in the most favorable in terms of total energy rodlike globular structure.

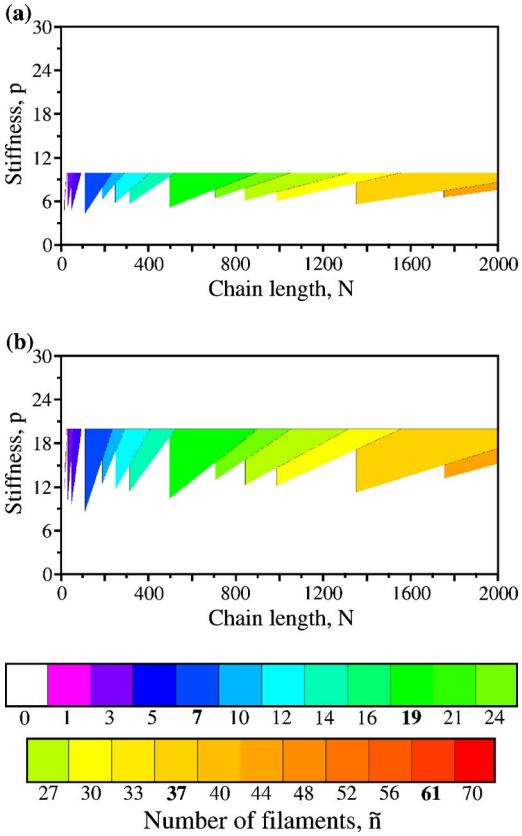

FIG. 12. (Color online) The maps of stability of perfect rodlike structures (with trivial bends) in variables of the chain length—stiffness for stiffness potential $U_\vartheta \sim \vartheta^2$, $\gamma=1.0$ (a), $\gamma=2.0$ (b). The color indicates the number of filaments in the most favorable in terms of total energy rodlike globular structure.

$$E_{\text{total}}^{\text{rod}} = n'\left[U_\vartheta\left(\frac{2\pi}{3}\right) + U_\vartheta\left(\frac{\pi}{3}\right)\right] + N\gamma\left(\frac{(\tilde{n}-n)}{\tilde{n}}A^{(n+1)} + \frac{[1-(\tilde{n}-n)]}{\tilde{n}}A^{(n)}\right) + 2n\gamma. \quad (14)$$

As for toroidal globule for a rodlike one we should also choose a criterion to distinguish it from an ellipsoidal globule. For such a criterion we choose the ratio of globule length H to its diameter d. If $\frac{H}{d}>3$ we call such a structure rodlike globule or rod. Otherwise we treat the structure as an ellipsoidal globule and do not consider it in our study. In terms of the number of monomers N and the number of filaments in the rod $\tilde{n}$ this criterion can be written in the following form:

$$\frac{N}{2\tilde{n}\sqrt{\tilde{n}}} > 3. \quad (15)$$

In Figures 11 and 12 we present the maps of stability of perfect rodlike structures in variables of the chain length—stiffness, $N-p$. As for the case of toroidal globule (see Fig. 3) by color we indicate the number of filaments in the most favorable perfect rodlike globule for particular chain length N, stiffness p, and surface tension γ. The upper limit in the stiffness parameter p is defined by the criterion $\gamma/p > (\gamma/p)^{\text{trivial}}$ described above.

It can be easily seen that in the case of rodlike structures in comparison to the case of toroids the maps built for $U_\vartheta \sim (1-\cos\vartheta)$ and for $U_\vartheta \sim \vartheta^2$ differ from each other. This is due to the fact that rodlike structures have sharp kinks in the chain direction. For bending on such angles the approximation $\cos\vartheta \approx 1-\frac{\vartheta^2}{2}$ is not valid, which leads to the pronounced difference in bending energy.

D. Comparison of stability of toroidal and rodlike globules

In this section we try to understand how the choice of a bending potential influences the volume fraction of toroidal and rodlike globules in the condensed state. We compare properties and energies of the most favorable toroid and rod (i.e., toroid and rod with smallest value of energy) for each particular chain length N and stiffness parameter p for both types of bending potentials: $U_\vartheta = f_1(1-\cos\vartheta)$ and $U_\vartheta = f_2\vartheta^2$.

Taking into account that the ratio of probabilities to get a rodlike or a toroidal conformation, $\frac{\rho_{\text{rod}}}{\rho_{\text{tor}}}$, is proportional to $\exp(-E_{\text{total}}^{\text{rod}} - E_{\text{total}}^{\text{tor}}/kT)$, we present maps not for energies themselves but rather for the difference $E_{\text{total}}^{\text{rod}} - E_{\text{total}}^{\text{tor}}$ for both bending potentials for the case of ideal toroid and perfect rod. As can be seen from Fig. 13 in the whole range of

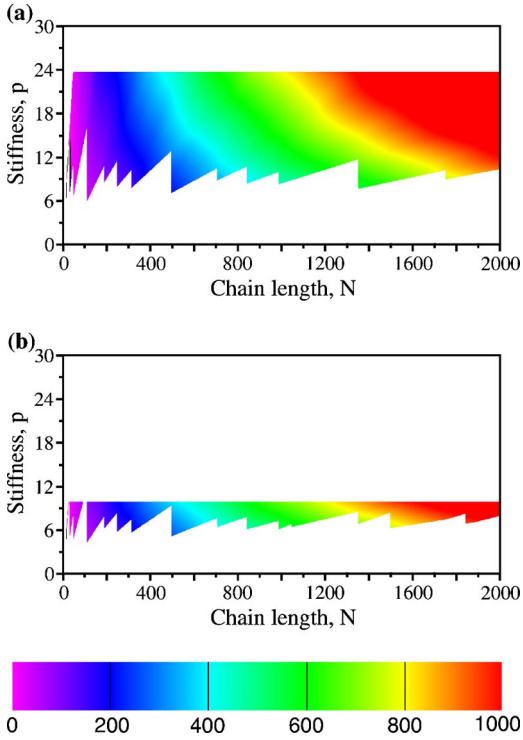

FIG. 13. (Color online) The maps of the difference in total energy between perfect rod and ideal toroid $E^{\mathrm{rod}}_{\mathrm{total}}(\mathrm{id})-E^{\mathrm{tor}}_{\mathrm{total}}(\mathrm{id})$. Bending potentials are $U_\vartheta \sim (1-\cos\vartheta)$ for the figure at the top and $U_\vartheta \sim \vartheta^2$ for the figure at the bottom, $\gamma=1.0$. Colors indicate the numerical values of the energy difference in kT.

parameters toroidal structure has lower energy than the corresponding rodlike one. This means that toroids are stable structures while rodlike globules are metastable ones. In terms of Monte Carlo simulation it means that the volume fraction of toroids is always larger than volume fraction of rodlike globules. Though the comparison has been performed for the case of ideal toroid and perfect rodlike globule the deviation due to nonideality of the structures cannot compensate the energy difference between the structures. We have calculated the difference in bending energy between perfect rod and nonideal toroid for toroids of 7, 19, 37, 61 circuits and found the trend to be the same as for the previous case.

IV. CONCLUSIONS

In this paper we have analyzed theoretically and numerically how the geometry of compact globular structures depends on the bending potential. It is well known that small globules formed by a semiflexible chain of finite length can take shapes of a torus, cylinder (rod), etc. Here, we have investigated two different globular structures, toroidal globule and rodlike one, for two different bending potentials: $U_\vartheta \sim (1-\cos\vartheta)$ and $U_\vartheta \sim \vartheta^2$. It has been shown that in the framework of the bead-stick model the number of filaments in toroidal and rodlike globules is a discrete function of the chain length and the stiffness. In order to understand this observation better we have built two-dimensional (2D) maps of stability for toroids and rods for both bending potentials. These maps show the number of filament in the toroidal or rodlike globule, respectively, which has the lowest energy at given values of chain length and stiffness.

We can conclude that the type of the bending potential influences both globular states. For the case of toroidal globule the type of the bending potential could be possibly recognized from the packing geometry of the filaments in toroid since the two potentials prefer different ground states (see Fig. 5). The difference in energy between two possible ground states becomes more pronounced with increasing the thickness of a toroid. For rodlike globules the shape of the bends does also depend very significantly on the particular bending potential (see Fig. 10). Namely, there are some values of the bend lengths which can be observed for the ϑ^2 potential only while they are not stable for the $\cos\vartheta$ potential. Decreasing the ratio of the surface tension and the stiffness parameter, γ/p, one would observe for ϑ^2 potential many possible intermediate shapes of loops consisting of a different number of beads, while there would be only a trivial bend followed by a sharp jump to a quite large loop of 11 beads for the $\cos\vartheta$ potential.

In order to understand which of these two structures (toroids or rodlike globules) is the stable one we have calculated the difference between energies $E^{\mathrm{rod}}_{\mathrm{total}}-E^{\mathrm{tor}}_{\mathrm{total}}$ for $U_\vartheta \sim (1-\cos\vartheta)$ and $U_\vartheta \sim \vartheta^2$. For all parameters considered here toroids were found to be the most favorable structure, while numerically its preference depends on the bending potential.

Summarizing, our main results are (1) the shape of the bending potential could be possibly seen from the geometry of a globule; (2) toroidal globules are always more favorable than the rodlike ones.

ACKNOWLEDGMENTS

The authors acknowledge stimulating discussions with A. Grosberg, V. Rostiashvili, and D. Andrienko and the financial support from Alexander von Humboldt Foundation and RFBR (Grant No. 06-03-33146).

[1] S. F. Sun, *Physical Chemistry of Macromolecules* (Wiley, Hoboken, NJ, 2004).
[2] H. Schiessel, J. Phys.: Condens. Matter **15**, R699 (2003).
[3] D. Luo and W. M. Saltzman, Nat. Biotechnol. **18**, 33 (2000).
[4] V. A. Bloomfield, Curr. Opin. Struct. Biol. **6**, 334 (1996).
[5] N. V. Hud, M. J. Allen, K. H. Downing, J. Lee, and R. Balhorn, Biochem. Biophys. Res. Commun. **193**, 1347 (1993).
[6] M. R. Shen, K. H. Downing, R. Balhorn, and N. V. Hud, J. Am. Chem. Soc. **122**, 4833 (2000).
[7] N. V. Hud and K. H. Downing, Proc. Natl. Acad. Sci. U.S.A. **98**, 14925 (2001).
[8] C. C. Conwell and N. V. Hud, Biochemistry **43**, 5380 (2004).

[9] A. A. Zinchenko, V. G. Sergeyev, S. Murata, and K. Yoshikawa, J. Am. Chem. Soc. **125**, 4414 (2003).
[10] H. Noguchi, S. Saito, S. Kidoaki, and K. Yoshikawa, Chem. Phys. Lett. **261**, 527 (1996).
[11] G. Maurstad and B. T. Stokke, Biopolymers **74**, 199 (2004).
[12] S. Danielsen, K. M. Varum, and B. T. Stokke, Biomacromolecules **5**, 928 (2004).
[13] G. Maurstad and B. T. Stokke, Curr. Opin. Colloid Interface Sci. **10**, 16 (2005).
[14] A. R. Khokhlov and A. Y. Grosberg, Adv. Polym. Sci. **41**, 53 (1981).
[15] A. Y. Grosberg, Biofizika **24**, 32 (1979).
[16] A. Y. Grosberg and A. V. Zhestkov, J. Biomol. Struct. Dyn. **3**, 859 (1986).
[17] J. Ubbink and T. Odijk, Biophys. J. **68**, 54 (1995).
[18] T. Odijk, Macromolecules **16**, 1340 (1983).
[19] T. Odijk, J. Chem. Phys. **105**, 1270 (1996).
[20] K. Yoshikawa, M. Takahashi, V. V. Vasilevskaya, and A. R. Khokhlov, Phys. Rev. Lett. **76**, 3029 (1996).
[21] Y. A. Kuznetsov, E. G. Timoshenko, and K. A. Dawson, J. Chem. Phys. **104**, 336 (1996).
[22] Y. A. Kuznetsov, E. G. Timoshenko, and K. A. Dawson, J. Chem. Phys. **105**, 7116 (1996).
[23] J. N. Bright and D. R. M. Williams, Europhys. Lett. **45**, 321 (1999).
[24] G. G. Pereira and D. R. M. Williams, Europhys. Lett. **50**, 559 (2000).
[25] Y. Ishimoto and N. Kikuchi, cond-mat/0507477 (unpublished).
[26] H. Noguchi and K. Yoshikawa, Chem. Phys. Lett. **278**, 184 (1997).
[27] H. Noguchi and K. Yoshikawa, J. Chem. Phys. **109**, 5070 (1998).
[28] Y. A. Kuznetsov and E. G. Timoshenko, J. Chem. Phys. **111**, 3744 (1999).
[29] U. Bastolla and P. Grassberger, J. Stat. Phys. **89**, 1061 (1997).
[30] F. Ganazzoli, Macromol. Theory Simul. **6**, 351 (1997).
[31] V. A. Ivanov, W. Paul, and K. Binder, J. Chem. Phys. **109**, 5659 (1998).
[32] V. A. Ivanov, M. R. Stukan, V. V. Vasilevskaya, W. Paul, and K. Binder, Macromol. Theory Simul. **9**, 488 (2000).
[33] M. R. Stukan, V. A. Ivanov, A. Y. Grosberg, W. Paul, and K. Binder, J. Chem. Phys. **118**, 3392 (2003).
[34] J. A. Martemyanova, M. R. Stukan, V. A. Ivanov, M. Müller, W. Paul, and K. Binder, J. Chem. Phys. **122**, 174907 (2005).
[35] T. Sakaue and K. Yoshikawa, J. Chem. Phys. **117**, 6323 (2002).
[36] T. Sakaue, J. Chem. Phys. **120**, 6299 (2004).
[37] I. R. Cooke and D. R. M. Williams, Physica A **339**, 45 (2004).
[38] B. Schnurr, F. C. MacKintosh, and D. R. M. Williams, Europhys. Lett. **51**, 279 (2000).
[39] B. Schnurr, F. Gittes, and F. C. MacKintosh, Phys. Rev. E **65**, 061904 (2002).
[40] A. Baumgärtner, *Applications of the Monte Carlo Method in Statistical Physics* (Springer, Berlin, 1987), p. 145.
[41] T. E. Cloutier and J. Widom, Mol. Cell **14**, 355 (2004).
[42] P. A. Wiggins, R. Phillips, and P. C. Nelson, Phys. Rev. E **71**, 021909 (2005).
[43] J. DeRouchey, R. R. Netz, and J. O. Rädler, Eur. Phys. J. E **16**, 17 (2005).
[44] I. M. Kulić, D. Andrienko, and M. Deserno, Europhys. Lett. **67**, 418 (2004).
[45] N. V. Hud, K. H. Downing, and R. Balhorn, Proc. Natl. Acad. Sci. U.S.A. **92**, 3581 (1995).
[46] K. A. Marx and G. C. Ruben, Nucleic Acids Res. **11**, 1839 (1983).
[47] S. Y. Park, D. Harries, and W. M. Gelbart, Biophys. J. **75**, 714 (1998).